

Controlling flow direction in nanochannels by electric field strength

Xiang Gao, Tianshou Zhao,* and Zhigang Li†

Department of Mechanical and Aerospace Engineering, The Hong Kong University of Science and Technology, Clear Water Bay, Kowloon, Hong Kong

(Received 18 May 2015; published 17 August 2015)

Molecular dynamics simulations are conducted to study the flow behavior of CsF solutions in nanochannels under external electric fields E . It is found that the channel surface energy greatly affects the flow behavior. In channels of high surface energy, water molecules, on average, move in the same direction as that of the electric field regardless of the strength of E . In low surface energy channels, however, water transports in the opposite direction to the electric field at weak E and the flow direction is changed when E becomes sufficiently large. The direction change of water flow is attributed to the coupled effects of different water-ion interactions, inhomogeneous water viscosity, and ion distribution changes caused by the electric field. The flow direction change observed in this work may be employed for flow control in complex micro- or nanofluidic systems.

DOI: [10.1103/PhysRevE.92.023017](https://doi.org/10.1103/PhysRevE.92.023017)

PACS number(s): 47.61.-k, 82.39.Wj, 82.45.-h

I. INTRODUCTION

High surface-area-to-volume ratio and fluid-wall interactions can lead to rich fluid flow scenarios at the nanoscale [1–3] and bring about considerable applications of nanofluidics in biology, medicine, and engineering, including DNA sorting, molecular separation, and chip-level cooling [4–7]. Lab-on-a-chip technology is a particular area that significantly benefits from the advances of micro- and nanofluidics. In many lab-on-a-chip systems, the flows of different streams need to be manipulated in a desired way to perform preferred mixing, reaction, and separation [8–10]. In certain cases, the control of the flow direction is of great importance. Due to the standard fabrication and simple operation, electroosmotic flows have been widely used in micrototal analysis systems [11–14]. In simple electroosmotic fluidic systems, the flow direction can be freely controlled by altering the direction of the external electric field. It can also be managed by changing the zeta potential between the fluid and channel [15–16], pH value of the fluid [17], or through the chemical modification of channel surfaces [18]. However, these flow regulation methods are generally global and may not be easily implemented in complex fluidic systems, especially when local flow regulation is required.

In this work, we propose a method to control the flow direction in nanochannels by changing the strength, instead of the direction, of the external electric field. The idea is based on the distinct fluid-cation and fluid-anion interactions, nonuniform fluid viscosity distribution, and the dependence of ion distribution on the electric field. Through molecular dynamics (MD) simulations, we investigate the water motion of a CsF solution in nanochannels by varying the external electric field strength. It is found that the channel surface energy greatly affects the water flow. In high surface energy channels (hydrophilic, strong fluid-wall interaction), water molecules always move in the same direction as the electric field regardless of the strength of the electric field. In channels of low surface energy (hydrophobic, weak fluid-wall

interaction), however, the direction of the water flow changes from negative (opposite to the electric field) to positive as the external electric field is strengthened.

II. MOLECULAR DYNAMICS SIMULATIONS

Molecular dynamics simulations are performed using the LAMMPS package [19]. The simulation system consists of a slit nanochannel formed by two parallel solid walls. The lengths of the channel are 6.1, 1.9, and 12.3 nm in the x , y , and z directions, respectively, as shown in Fig. 1. Each channel wall contains four layers of atoms, which are initially on face-centered cubic lattice sites with a lattice constant equal to 4.09 Å. The outer two layers are fixed to stabilize the channel, while the atoms of the two inner layers are free to vibrate to consider the flexibility of the channel and control the temperature of the system. The embedded atom method potential with parameters for silver is employed to simulate the walls [20]. The channel is filled with a CsF solution containing 4104 water molecules and 171 pairs of Cs⁺ and F[−] ions randomly distributed in water. The center of the channel is located at $(x, y, z) = (0, 0, 0)$ and an external electric field is applied in the positive z direction. Water molecules are simulated with the simple point charge-extended (SPC/E) model [21] and ions are treated as charged Lennard-Jones (LJ) particles. Each oxygen and hydrogen atom carries a point charge q equal to $-0.8476 e$ and $0.4238 e$, respectively. Cs⁺ and F[−] hold a unit charge. The water-water and water-ion interactions are modeled by combining the LJ and Coulomb potentials [22]

$$U = \sum_i \sum_j \left\{ 4\varepsilon_{ij} \left[\left(\frac{\sigma_{ij}}{r_{ij}} \right)^{12} - \left(\frac{\sigma_{ij}}{r_{ij}} \right)^6 \right] + \frac{q_i q_j}{r_{ij}} \right\}, \quad (1)$$

where ε_{ij} and σ_{ij} are the binding energy and collision diameter for the interacting water molecules or ions i and j , and r_{ij} is the separation distance. The LJ potential is employed to describe the interactions between the wall atoms and water molecules or ions, which has been shown to be reasonable for uncharged walls [14,22,23]. The LJ parameters $\varepsilon_{\alpha\beta}$ and $\sigma_{\alpha\beta}$ for different species α and β are obtained by using the Lorentz-Berthelot mixing rule [3] $\sigma_{\alpha\beta} = (\sigma_{\alpha\alpha} + \sigma_{\beta\beta})/2$ and

*metzhao@ust.hk

†mezli@ust.hk

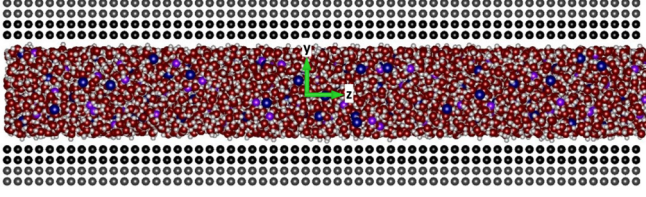


FIG. 1. (Color online) A snapshot of the MD simulation system (O: red; H: white; Cs⁺: blue; F⁻: purple). Electric field E is applied in the positive z direction.

$\varepsilon_{\alpha\beta} = \sqrt{\varepsilon_{\alpha\alpha}\varepsilon_{\beta\beta}}$, based on the self-interaction parameters given in Refs. [21] and [24]. To consider the wall effects and apply this mixing rule, the self-interacting binding energy for the wall atoms ε_{ww} is varied artificially in a wide range. Such that the interaction strength between water molecules and ions and the channel is adjusted, which is equivalent to change the surface free energy of the channel [2,25,26]. All the parameters used for the potentials are given in Table I.

The simulations are carried out in a $61.3 \times 136.2 \times 122.7 \text{ \AA}^3$ cell with periodic boundary conditions (PBCs) in all directions. The SHAKE algorithm is adopted to constrain the \angle HOH angles and O–H bonds in water molecules. The cutoff distance for the LJ and Coulomb potentials is set as 1 nm. The particle-particle particle-mesh method is used to account for the long-range Coulombic forces. The temperature of the system is maintained at 300 K by applying the Berendsen thermostat to the degrees of freedom of water molecules and ions in the x and y directions. The time step is 1 fs. The system is relaxed for 5 ns after the initialization. Then an external electric field is applied in the positive z direction and another 5-ns relaxation is performed, which is followed by the data collection for 30–60 ns.

To understand the flow in nanochannels, the water motion in bulk solutions is also studied. In this case, 3115 water molecules and 130 pair of Cs⁺ and F⁻ ions are filled in a cubic cell of side length equal to 4.7 nm with PBCs in all directions. The system is relaxed for 1 ns first and then an external electric field is applied. Water velocity is obtained after another 1-ns relaxation. The other simulation parameters are the same as those in the confined cases.

III. RESULTS AND DISCUSSION

We first investigate the water motion in bulk solutions without confinements. As the external electric field strength E is varied, the mean velocity of water molecules \bar{V} is obtained,

TABLE I. Potential parameters in MD simulations.

Atoms	σ (Å)	ε (K)	Charge (e)
O	3.166	78.2	-0.8476
H	0.0	0.0	0.4238
Cs ⁺	3.883	50.3	1.0
F ⁻	3.117	90.6	-1.0
Wall atoms	3.4	ε_{ww} (adjustable)	0.0

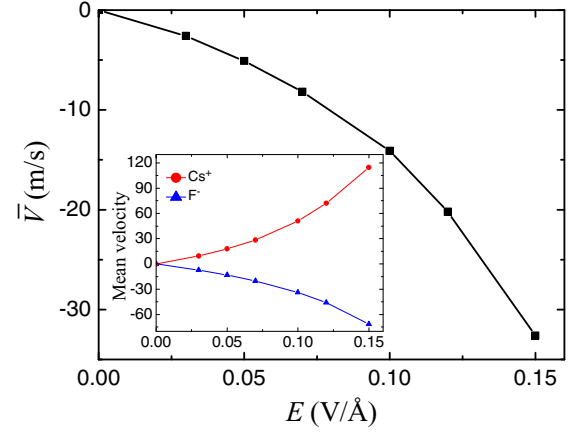


FIG. 2. (Color online) Mean velocity of water \bar{V} versus electric field E in bulk solutions. The inset shows the mean velocities of F⁻ and Cs⁺.

which is computed as

$$\bar{V} = \frac{\int_y v_z(y)\rho(y)dy}{\int_y \rho(y)dy}, \quad (2)$$

where v_z and ρ are the local velocity in the z direction and number density of water molecules. Figure 2 shows \bar{V} as a function of E . It is seen that the water molecules always move in the negative direction (opposite to the electric field) and the speed increases with increasing electric field strength. This is not surprising in bulk solutions given the difference between the water-F⁻ and water-Cs⁺ interaction strengths. For water-ion interactions, it is known that water molecules surrounding an ion usually form an ionic hydration shell due to the relatively strong water-ion binding energy [22]. The average potential energy between the ion and the water molecules in the hydration shell is called hydration energy. The water-F⁻ hydration energy is -141.3 Kcal/mol , which is much stronger than that between water and Cs⁺ (-46.4 Kcal/mol) because F⁻ has higher charge density than that of Cs⁺ due to its small size. This leads to the formation of a relatively stable ionic hydration shell around each F⁻ ion [22]. Therefore, as F⁻ ions move under the electric field, they carry more water molecules than do Cs⁺ ions. Although F⁻ ions have lower speeds than Cs⁺ [24], as shown in the inset of Fig. 2, water molecules on average travel in the same direction as F⁻ ions, opposite to the electric field. The moving direction of water can also be explained on the basis of momentum conservation. Since the total force acting on the system (ions and water molecules) is zero, water molecules have to move in the same direction as F⁻ to make the momentum of the whole system vanish as Cs⁺ moves faster than F⁻ due to the small drag coefficient [24]. Hence, in bulk solutions, the strong water-F⁻ interaction plays a dominant role and brings water molecules to move with F⁻ in the direction opposite to the electric field.

In nanochannels, the water motion can be different due to surface effects. The mean velocity of water molecules in nanochannels of different surface energies is depicted in Fig. 3 as E is varied. At relatively low surface energies $\varepsilon_{ww} = 50$ and 100 K, for which the channel surface is hydrophobic with water

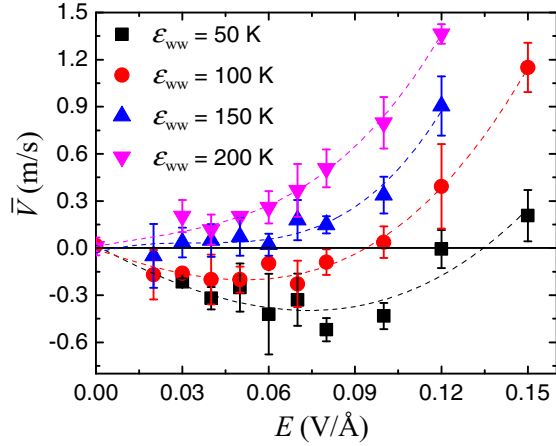


FIG. 3. (Color online) Mean velocity of water \bar{V} as a function of electric field E in channels of different surface energies. Dashed lines are a guide to the eye.

contact angle $\theta \approx 120^\circ$ and $\theta \approx 110^\circ$, respectively [25], it is seen that the flow direction of water is altered as the external electric field strength is increased. For relatively weak electric fields, the water velocity \bar{V} is negative (opposite to the electric field) and assumes the maximum as E is increased. When E becomes sufficiently large, the flow direction changes from negative to positive. For intermediate surface energy $\varepsilon_{\text{ww}} = 150 \text{ K}$, the flow direction change is unobservable. At high surface energy $\varepsilon_{\text{ww}} = 200 \text{ K}$, however, water molecules always move in the same direction as the electric field, as shown in Fig. 3.

The distinct flow behaviors in different channels are caused by the coupled effects of several factors, including water-ion interactions, ion distributions, and the inhomogeneous physical properties of water (especially viscosity), as E is changed. As introduced previously, water- F^- interaction is stronger than that between water and Cs^+ . Therefore, compared to Cs^+ ions, F^- ions can carry more water molecules as they migrate. The F^- and Cs^+ distributions in the channel are also different. Figure 4 depicts the density distributions of F^- and Cs^+ under various conditions (a detailed discussion will be presented later). It is found that generally the concentration of F^- is higher than that of Cs^+ near the channel surface and around the center, and the majority of Cs^+ ions are in the area between the center and channel surface ($y = \pm 4.5 \text{ \AA}$) no matter how E and the surface property are varied. This is the consequence of ion-wall interactions (F^- -wall interaction is stronger than Cs^+ -wall interaction) and that among the ions. For the water property changes, it has been shown that fluids in nanoconfinements exhibit nonuniform density and viscosity distributions [1,27,28]. Figure 5 illustrates the number density and viscosity of pure water in the channel (viscosity is calculated following the approach in Ref. [29]). It is seen that density [Fig. 5(a)] and viscosity [Fig. 5(b)] share a similar distribution. They are higher near the channel surface than those around the center due to the wall effects, which are consistent with previous work [1,27–29]. Given these static properties, the flow patterns in Fig. 3 can be easily understood.

In low surface energy channels, for instance, $\varepsilon_{\text{ww}} = 100 \text{ K}$ in Fig. 3, the wall effect is weak and the total force acting

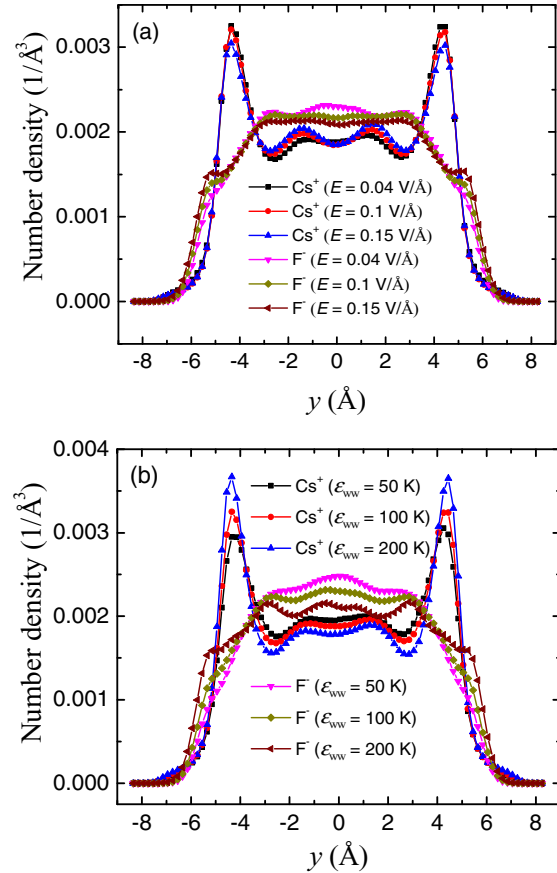


FIG. 4. (Color online) Number density distributions of F^- and Cs^+ . (a) In the channel of $\varepsilon_{\text{ww}} = 100 \text{ K}$ for different electric field strengths. (b) $E = 0.04 \text{ V/\AA}$ for different ε_{ww} values.

on the system by the channel is negligible at relatively weak electric fields. In this case, the transport of water molecules and ions is similar to that in bulk solutions. As E is increased, F^- ions carry more water molecules moving in the negative direction and the water speed increases as the electric field is enhanced (Fig. 3). Figure 6(a) depicts the velocity profiles of water as a function of E . As E is changed from 0.02 to 0.04 V/\AA , the magnitude of water velocity around the center increases and is the major contribution to the water flow. The negative water velocity in the center region is caused by the motion of F^- , which is consistent with the F^- distribution, as shown in Fig. 4(a). As the electric field is further increased, higher than 0.04 V/\AA , however, the flow speed is reduced and then the flow direction is changed to positive when E is larger than 0.1 V/\AA . This is caused by the ion distribution change. As depicted in Fig. 4(a), as the electric field is strengthened, F^- ions tend to move toward the surface, while Cs^+ ions migrate to the center region. Since the water viscosity near the channel surface is much larger than that in the center region [Fig. 5(b)], the ion distribution change induced by the increasing electric field greatly reduce the velocity increase of F^- near the surface, while enhancing the transport of water molecules in the positive direction caused by the motion of Cs^+ ions, as shown in Fig. 6(a). Therefore, the nonlinear behavior of water transport and flow direction change in hydrophobic channels ($\varepsilon_{\text{ww}} = 50$ and 100 K in Fig. 3) are

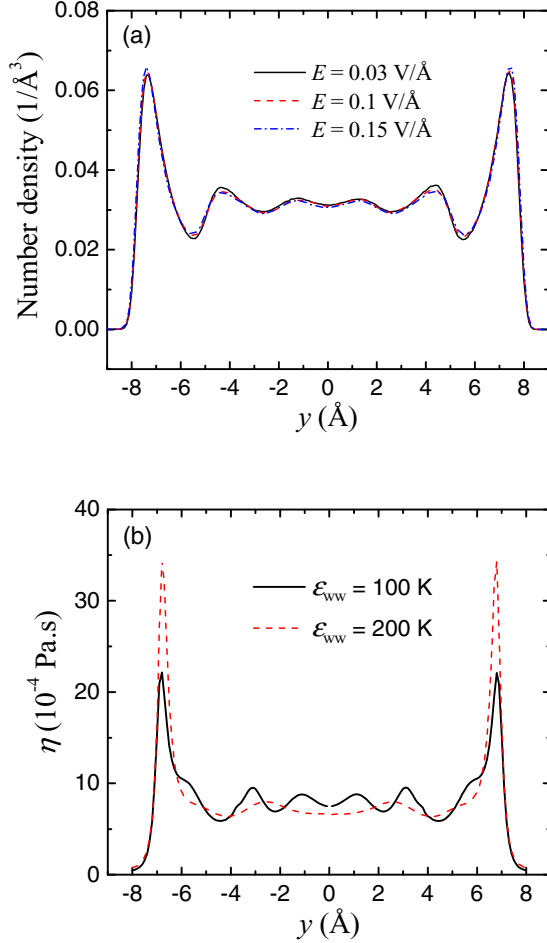


FIG. 5. (Color online) Water property change in the channel. (a) Density distribution for $\epsilon_{\text{ww}} = 100 \text{ K}$ at different electric field strengths. (b) Viscosity change of pure water in channels of $\epsilon_{\text{ww}} = 100$ and 200 K without external electric field.

caused by the competition between two effects as the electric field is strengthened. One is the motion of F^- ions in the negative direction, which drive many water molecules to move opposite to the electric field. The other is the increasing friction coefficient for F^- ions as they migrate toward the channel surface as E is strengthened, which reduces the velocity of F^- . The coupled effects make the water flow assume the maximum velocity at certain electric field strength. For $\epsilon_{\text{ww}} = 50 \text{ K}$, the wall effect is even weaker and the electric field strength for the maximum flow velocity is 0.08 V/\AA , higher than 0.04 V/\AA for the channel of $\epsilon_{\text{ww}} = 100 \text{ K}$, as shown in Fig. 3.

In high surface energy channels, both water-wall and ion-wall interactions become strong. The former increases the water viscosity near the channel surface and the latter attracts both F^- and Cs^+ ions toward the surface, as depicted in Figs. 5(b) and 4(b), respectively. Hence, the motion of F^- ions is hindered and the water flow is dominated by the transport of Cs^+ ions, as confirmed by the water velocity profiles in different channels at $E = 0.04 \text{ V/\AA}$ in Fig. 6(b). This is why water molecules, on average, move in the direction of the electric field and flow direction change does not occur for $\epsilon_{\text{ww}} = 200 \text{ K}$ in Fig. 3.

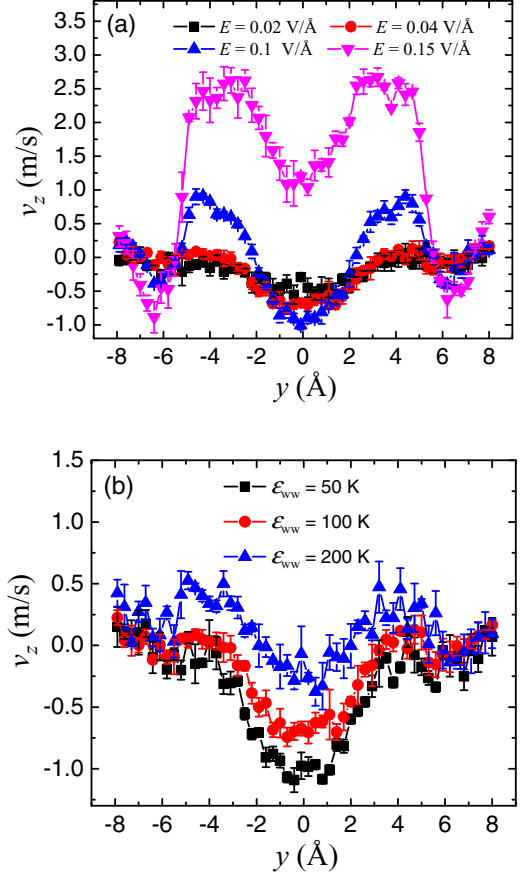


FIG. 6. (Color online) Velocity profiles of water in the channel. (a) $\epsilon_{\text{ww}} = 100 \text{ K}$ under different electric field strengths. (b) $E = 0.04 \text{ V/\AA}$ for $\epsilon_{\text{ww}} = 50, 100,$ and 200 K .

As the channel surface plays an important role, the channel height is expected to affect the water velocity and it is reasonable to assume that there is a critical channel height, above which flow direction change will not be observed. This is beyond the scope of current work. Nevertheless, simulations in a 3.9-nm -high channel for $\epsilon_{\text{ww}} = 100 \text{ K}$ are also performed (not reported here), and as expected, water molecules tend to move with a higher velocity in the direction opposite to the electric field compared with that in the 1.9 nm channel, approaching the case in bulk solutions.

The impeded motion of F^- ions due to the viscous effects at strong E can also be described by the Navier-Stokes equation in the flow direction by considering the nonuniform viscosity distribution, which reads

$$\frac{\partial^2 v_z(y)}{\partial y^2} = -\frac{E \rho_e(y)}{\eta(y)}, \quad (3)$$

where $\rho_e(y) = e[\rho_{\text{Cs}^+}(y) - \rho_{\text{F}^-}(y)]$ is the local net charge density. By using $\rho_e(y)$ and $\eta(y)$ obtained through MD simulations, together with the boundary conditions, $\partial v_z / \partial y|_{y=0} = 0$ and $v_z = 0$ at channel surfaces, Eq. (3) is solved for $\epsilon_{\text{ww}} = 100 \text{ K}$ and the results are shown in Fig. 7. Generally, the velocity profiles at different electric fields are similar to the MD results in Fig. 6(a). This verifies that the water flow direction change under strong E is caused by the ion distribution change and enhanced viscosity at the channel surface. The discrepancy

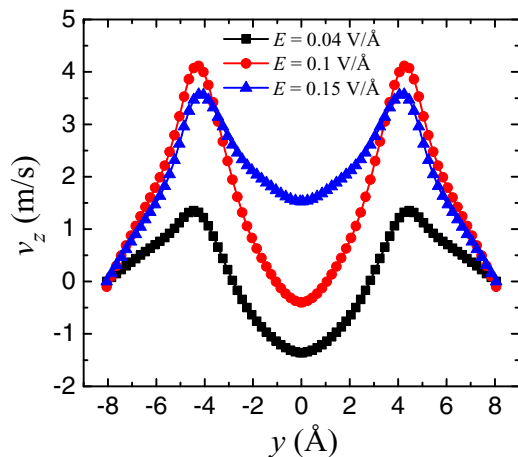


FIG. 7. (Color online) Numerical results of Eq. (3) for water velocity at $\varepsilon_{\text{ww}} = 100$ K under different electric field strengths.

between Eq. (3) and the MD results is mainly caused by the water-ion interactions, which are important, but cannot be considered in Eq. (3). The numerical error in viscosity calculation due to the small size of the channel may also contribute to the discrepancy.

IV. CONCLUSION

We have investigated the water motion of CsF solutions under external electric fields in nanochannels. It is found that the water flow strongly depends on the channel surface property. In channels of low surface energy, the flow direction of water can be altered by varying the strength of the electric field E . Under weak electric fields, water molecules, on average, move in the opposite direction to E mainly due to the motion of F^- ions. However, the flow direction is changed when the electric field becomes sufficiently strong. The flow direction change is caused by the migration of F^- ions toward the surface as the electric field is strengthened, which makes the transport of Cs^+ dominant. The findings in this work may provide new insights and methods for the flow control in complex nanofluidic systems.

ACKNOWLEDGMENTS

This work was supported by the Collaborative Research Fund of the Hong Kong Special Administrative Region under Grant No. HKUST9/CRF/11G. X.G. was partially supported by a Postgraduate Scholarship through the Energy Technology Concentration at HKUST.

-
- [1] C. Liu and Z. G. Li, *Phys. Rev. E* **80**, 036302 (2009).
 - [2] C. Liu and Z. G. Li, *Phys. Rev. Lett.* **105**, 174501 (2010).
 - [3] Z. G. Li, *Phys. Rev. E* **79**, 026312 (2009).
 - [4] T. M. Squires and S. R. Quake, *Rev. Mod. Phys.* **77**, 977 (2005).
 - [5] L. Bocquet and E. Charlaix, *Chem. Soc. Rev.* **39**, 1073 (2010).
 - [6] J. Fu, R. B. Schoch, A. L. Stevens, S. R. Tannenbaum, and J. Han, *Nat. Nanotechnol.* **2**, 121 (2007).
 - [7] S. K. Min, W. Y. Kim, Y. Cho, and K. S. Kim, *Nat. Nanotechnol.* **6**, 162 (2011).
 - [8] C.-C. Chang and R.-J. Yang, *Microfluid Nanofluid* **3**, 501 (2007).
 - [9] I. Shestopalov, J. D. Tice, and R. F. Ismagilov, *Lab Chip* **4**, 316 (2004).
 - [10] N. Pamme, *Lab Chip* **7**, 1644 (2007).
 - [11] R. Sadr, M. Yoda, Z. Zheng, and A. T. Conlisk, *J. Fluid Mech.* **506**, 357 (2004).
 - [12] S. J. Kim, Y. C. Wang, J. H. Lee, H. Jang, and J. Han, *Phys. Rev. Lett.* **99**, 044501 (2007).
 - [13] R. Qiao and N. R. Aluru, *J. Chem. Phys.* **118**, 4692 (2003).
 - [14] D. M. Huang, C. Cottin-Bizonne, C. Ybert, and L. Bocquet, *Phys. Rev. Lett.* **98**, 177801 (2007).
 - [15] L. C. Chen, C. C. Wu, R. G. Wu, and H. C. Chang, *Langmuir* **28**, 11281 (2012).
 - [16] Y. J. Oh, T. C. Gamble, D. Leonhardt, C. H. Chung, S. R. J. Brueck, C. F. Ivory, G. P. Lopez, D. N. Petsev, and S. M. Han, *Lab Chip* **8**, 251 (2008).
 - [17] M. A. Hayes, I. Kheterpal, and A. G. Ewing, *Anal. Chem.* **65**, 27 (1993).
 - [18] S. L. R. Barker, D. Ross, M. J. Tarlov, M. Gaitan, and L. E. Locascio, *Anal. Chem.* **72**, 5925 (2000).
 - [19] S. Plimpton, *J. Comp. Phys.* **117**, 1 (1995).
 - [20] S. M. Foiles, M. I. Baskes, and M. S. Daw, *Phys. Rev. B* **33**, 7983 (1986).
 - [21] H. J. C. Berendsen, J. R. Grigera, and T. P. Straatsma, *J. Phys. Chem.* **91**, 6269 (1987).
 - [22] X. Gao, T. S. Zhao, and Z. G. Li, *J. Appl. Phys.* **116**, 054311 (2014).
 - [23] D. Kim and E. Darve, *J. Colloid Interface Sci.* **330**, 194 (2009).
 - [24] S. Koneshan, J. C. Rasaiah, R. Lynden-Bell, and S. Lee, *J. Phys. Chem. B* **102**, 4193 (1998).
 - [25] J. W. Mo, L. Li, J. F. Zhou, D. Y. Xu, B. L. Huang, and Z. G. Li, *Phys. Rev. E* **91**, 033022 (2015).
 - [26] C. Liu, Y. Lv, and Z. G. Li, *J. Chem. Phys.* **136**, 114506 (2012).
 - [27] B. D. Todd, D. J. Evans, and P. J. Daivis, *Phys. Rev. E* **52**, 1627 (1995).
 - [28] C. Liu and Z. G. Li, *AIP Adv.* **1**, 032108 (2011).
 - [29] M. Predota, P. T. Cummings, and D. J. Wesolowski, *J. Phys. Chem. C* **111**, 3071 (2007).